



Published in final edited form as:

Environ Sci Technol. 2010 October 1; 44(19): 7309–7314. doi:10.1021/es100417s.

Dispersion and Stability Optimization of TiO₂ Nanoparticles in Cell Culture Media

Zhaoxia Ji[†], Xue Jin[‡], Saji George^{†, #}, Tian Xia^{†, #}, Huan Meng^{†, #}, Xiang Wang^{†, #}, Elizabeth Suarez^{†, ¶}, Haiyuan Zhang^{†, #}, Eric M.V. Hoek^{†, ‡}, Hilary Godwin^{†, ¶}, André E. Nel^{†, #}, and Jeffrey I. Zink^{†, §, *}

[†]California NanoSystems Institute, University of California at Los Angeles, Los Angeles, CA 90095, USA

[‡]Department of Civil & Environmental Engineering, University of California at Los Angeles, Los Angeles, CA 90095, USA

[#]Department of Medicine-Division of NanoMedicine, University of California at Los Angeles, Los Angeles, CA 90095, USA

[¶]Department of Environmental Health Sciences, University of California at Los Angeles, Los Angeles, CA 90095, USA

[§]Department of Chemistry and Biochemistry, University of California at Los Angeles, Los Angeles, CA 90095, USA

Abstract

Accurate evaluation of engineered nanomaterial toxicity requires not only comprehensive physical-chemical characterization of nanomaterials as produced, but also thorough understanding of nanomaterial properties and behavior under conditions similar to those used for *in vitro* and *in vivo* toxicity studies. In this investigation, TiO₂ nanoparticles were selected as a model nanoparticle and bovine serum albumin (BSA) was selected as a model protein for studying the effect of protein-nanoparticle interaction on TiO₂ nanoparticle dispersion in six different mammalian, bacteria, and yeast cell culture media. Great improvement in TiO₂ dispersion was observed upon the addition of BSA, even though the degree of dispersion varied from medium to medium and phosphate concentration in the cell culture media was one of the key factors governing nanoparticle dispersion. Fetal bovine serum (FBS) was an effective dispersing agent for TiO₂ nanoparticles in all six media due to synergistic effects of its multiple protein components, successfully reproduced using a simple “FBS mimic” protein cocktail containing similar concentrations of BSA, γ -globulin, and apo-transferrin.

Keywords

Titanium Dioxide; Nanoparticle Dispersion; Stability; Bovine Serum Albumin; Fetal Bovine Serum; Cell Culture Media

*Corresponding author: Department of Chemistry and Biochemistry, University of California, Los Angeles, 405 Hilgard Ave., Los Angeles, CA 90095; phone: (310) 825-1001; fax: (310) 206-4038, zink@chem.ucla.edu.

Supporting Information Available

Information on physical-chemical characterization techniques, TiO₂ nanoparticle dispersion in cell culture media with or without dispersing agents (Figure S1), dispersion and stability characterization methods, water chemistry analyses (Table S1), and UV-vis sedimentation study of TiO₂ nanoparticles in cell culture media (Figure S2). This information is available free of charge via the Internet at <http://pubs.acs.org>.

Introduction

With the increasing use of commercial nanomaterials in many consumer products, it is critical to identify potential impacts of nanomaterials on human health and the environment (1). The distribution of nanomaterials in the environment is governed by modes of release, physical-chemical properties of nanoparticles, and their interactions with biological substrates. Complete risk and safety assessment requires comprehensive physical-chemical characterization of the nanomaterials including chemical composition, size, morphology, surface area, crystallinity, and other physical-chemical properties (2). It is also very important to understand nanoparticle behavior under conditions similar to those for *in vitro* or *in vivo* nanotoxicity studies. It is well known that nanoparticles agglomerate immediately upon addition to cell culture media (3–5). If the agglomerates are used directly for nanotoxicity studies, it would result in inaccurate dose estimation and the interpretation of the toxicity results would be complicated (3). Based on these considerations, increasing attention is being paid to developing accurate methods for nanoparticle suspension preparation. Proteins, serum, and chemical surfactants are often used to enhance nanoparticle dispersion and stabilization (4, 6–12). Special attention should be paid when selecting a dispersing agent as it may interfere with nanotoxicity result interpretation. Surfactants such as sodium dodecyl sulfate or Tween 80 can be toxic. In comparison, nontoxic biologically relevant species would be the most promising candidates.

Bovine serum albumin (BSA) is the most abundant protein in blood plasma. It is believed that nanoparticles are covered by proteins immediately upon contact with a physiological environment, resulting in protein decoration also referred to as a protein corona on the particle surface (13, 14). Therefore BSA as a natural component in physiological fluid has been widely explored for dispersing various nanoparticles (4, 6–7). Fetal bovine serum (FBS) is another example of biologically relevant dispersing agent, which is often added as a growth supplement for various mammalian cell lines. Studies have shown that FBS at a typical concentration of 10% (v/v) can effectively improve nanoparticle dispersion in various media (8–12). Although all these studies were conducted in mammalian cultures, the same principles established for BSA and FBS can be also extended to the dispersion in bacteria and yeast media, which often contain other types of proteins.

One main objective of this investigation is to accurately evaluate particle size and state of dispersion in various commonly used cell culture media. Titanium dioxide (TiO₂) P25, one of the most widely used nanomaterials, was selected as a model nanoparticle. A systematic optimization of TiO₂ nanoparticle dispersion and stabilization in multiple types of media was also performed. Effort was made to identify and understand the potential mechanisms of BSA-nanoparticle interaction and the important parameters that affect such an interaction. The knowledge of these results on nanoparticle dispersion in different cell culture media will provide a valuable platform for studies of the environmental implications of nanomaterials.

Materials and Methods

Titanium dioxide P25 nanoparticles were received as dry powder. After detailed size, morphology, impurity, and surface area characterization (see Supporting Information for all characterization techniques), the sample was suspended in deionized water at a concentration of 1 mg mL⁻¹ to form a stock solution. Six different cell culture media including Bronchial Epithelial Growth Medium (BEGM), Dulbecco's Modified Eagle's Medium (DMEM), Luria Bertani Broth (LB), Tryptic Soy Broth (TSB), Synthetic Defined medium (SD), and Yeast Extract Peptone Dextrose medium (YPD) were selected for TiO₂ nanoparticle dispersion studies. A systematic water quality analysis was conducted for each medium. All characterization techniques were described in the Supporting information. High

throughput dynamic light scattering (HT-DLS, Dynapro™ Plate Reader, Wyatt Technology) was performed to determine the particle size distribution and state of agglomeration/dispersion of the nanoparticles in water and all different cell culture media. The plate reader is operated based on the same principles as the traditional DLS instruments but in a much more rapid manner. Analysis can be done using standard 96-, 384-, 1536-well plates. Since each measurement takes only a few seconds, ten runs were collected for each well and samples were loaded in at least triplicate. Particle sizes at various nanoparticle concentrations in all six media were determined simultaneously. Agglomeration kinetics measurements in each medium were conducted using the built-in kinetics feature in the HT-DLS instrument. This instrument provides a high throughput characterization method in parallel with the high throughput nanotoxicity studies. In addition to the dispersion characterization, the stability of the nanoparticle dispersions with or without dispersing agents was also evaluated by monitoring a characteristic peak of TiO₂ UV-vis absorbance spectrum as a function of time. Zeta potentials of the TiO₂ nanoparticle suspensions as another indication of the particle stability were also collected.

Results and Discussion

Physical-chemical Characterization of TiO₂ Nanoparticles

TEM analysis revealed the irregular morphology of the nanoparticles in the TiO₂ P25 sample. The primary particle size was estimated to be 20–30 nm from high resolution TEM analysis (Figure 1a). Lower magnification TEM analysis also showed the coexistence of larger TiO₂ agglomerates (Figure 1b). XRD analysis (Figure 1c) showed that TiO₂ P25 is composed of anatase and rutile. No other phase was detected. The phase composition was calculated to be 81 wt.% anatase and 19 wt.% rutile. Other physical-chemical properties such as BET surface area (51.5 m² g⁻¹), purity (98.03% TiO₂) of this material were also obtained, however no detailed discussion on these characterizations will be provided as the present investigation is mainly focused on particle size and dispersion characterization in water and cell culture media.

Water Chemistry Analysis of Cell Culture Media

A detailed water quality analysis of all six cell culture media is included as Table S1 in the Supporting Information. All six culture media had high ionic strength (50–270 mM) and conductivity (3–17 ms cm⁻¹). The main cations were Na⁺ and K⁺. The hardness, which was calculated based on Ca²⁺ and Mg²⁺ concentrations, appeared to be much higher in DMEM and SD media. PO₄³⁻, SO₄²⁻, Cl⁻ were detected as the main anions.

Direct Suspension of TiO₂ Nanoparticles

TiO₂ P25 nanoparticles suspended in deionized water at a 50 μg mL⁻¹ concentration formed a relatively stable dispersion with a zeta potential of 30.2 mV. Under the optimum sonication conditions, the particle size was ~200 nm. The much larger hydrodynamic diameter compared to the primary particle size suggests that the TiO₂ P25 sample consists of some hard aggregates that are not easily broken up by ultrasonication. Similar observations have also been made in some earlier studies (15, 16). When suspended in cell culture media without any dispersing agents, TiO₂ nanoparticles showed much poorer dispersion. High throughput DLS analysis of TiO₂ suspensions at a 50 μg mL⁻¹ concentration showed that the agglomerate size varied from 770 nm to 1052 nm depending on the type of medium (Table 1). Consistent with the dramatic size increase, the zeta potentials of all suspensions also dropped to ~ -10 mV (Table 1). The pHs remained similar to those of the nanoparticle-free media. Unlike in water where particle size remained similar in a wide range of nanoparticle concentrations (2 μg mL⁻¹ to 100 μg mL⁻¹), the TiO₂ agglomerate size increased with increasing nanoparticle concentration in all cell culture media (Figure 2).

The high ionic strengths (Table S1) in all cell culture media are probably one of the reasons for the severe TiO₂ nanoparticle agglomeration. According to Derjaguin, Landau, Verwey and Overbeek (DLVO) theory, the stability of a colloidal suspension is based on the net balance of two forces: the electrostatic repulsion which prevents aggregation and a universal attractive van der Waals force which acts to bind particles together (17, 18). In dilute electrolyte solutions, the counterion clouds that charge-compensate the charged surface of nanoparticles extend far from the particle surface making the double-layer interaction a long-range interaction. Since the van der Waals attraction is relatively weak at long range, electrostatic repulsion dominates and a stable nanoparticle suspension results. However, high ionic strength compresses the electrical double layer and the magnitude of the repulsive barrier decreases whereby van der Waals attraction dominates. Therefore, the net interaction potential becomes purely attractive at long and short range leading to nanoparticle agglomeration as observed in the cell culture media.

Improved TiO₂ Nanoparticle Dispersion with BSA or FBS

To improve the TiO₂ nanoparticle dispersion, BSA as a model protein and FBS as a protein rich serum were selected. The concentration of each dispersing agent was adjusted to achieve the best TiO₂ nanoparticle dispersion.

Effect of BSA on TiO₂ Nanoparticle Dispersion—Adsorption of protein molecules such as BSA onto nanoparticle surface could be achieved through electrostatic interaction, hydrophobic interaction, or specific chemical interaction (13, 19). The type of interaction between protein and nanoparticles strongly depends on pH and ionic strength of the media. In the present investigation, the isoelectric point (IEP) of BSA was ~4.7. At pH close to the IEP, BSA is hydrophobic and in its most compact form, thus the adsorption can occur through hydrophobic interactions. Above this pH, BSA becomes negatively charged and the electrostatic forces become dominant over hydrophobic interaction. Below the IEP, BSA is positively charged and similar electrostatic interaction can be expected. Since BSA is a macromolecule (hydrodynamic radius of ~7.5 nm by DLS), steric or electrosteric interactions may also play an important role during the nanoparticle dispersion.

High throughput DLS analysis results showed that, at a constant 50 µg mL⁻¹ TiO₂ nanoparticle concentration, 0.5 mg mL⁻¹ BSA was effective to reduce the agglomeration in most cell culture media (Figure 3). The optimum BSA concentration was determined to be 2 mg mL⁻¹ for achieving the best dispersion. The variation in TiO₂ nanoparticle dispersion from medium to medium could be attributed to the different water chemistry (Table S1) and therefore different adsorption mechanisms of BSA. In general, the maximum adsorption of BSA occurred around the IEP of BSA, in the pH range of 4–5 (20–24). In this pH range, lateral protein-protein electrostatic repulsive interaction is minimized; a close-packed monolayer of BSA molecules is usually formed via hydrophobic attraction (21, 22). Since the pH of SD medium (~4.6) falls in this range, hydrophobic interaction is expected to play an important role in the BSA adsorption and the consequent nanoparticle dispersion. In the case of YPD (pH ~5.9), BSA becomes negatively charged while TiO₂ particle surfaces still remain positively charged; BSA could be directly adsorbed onto nanoparticle surfaces by ionic interaction between carboxyl acid groups on BSA and the hydroxyl groups (–OH) on TiO₂ particle surface (20). In all other media including BEGM, DMEM, LB and TSB, both BSA and TiO₂ surface carry negative charges; high protein-protein and protein-TiO₂ nanoparticle repulsions are expected, and thus, protein adsorption should be severely reduced. This is a customary explanation for the low protein adsorption at high pH in aqueous solution (22). It is also consistent with the observed poor TiO₂ dispersion in LB and TSB. However, the fact that BSA greatly improved TiO₂ nanoparticle dispersion in BEGM and DMEM, where both BSA and TiO₂ are negatively charged, implies that mechanisms

other than simple electrostatic interaction might also play a role. The pH or surface charge alone could not explain the TiO₂ nanoparticle dispersion in all cell culture media.

Key Roles of Divalent Cations and Phosphate Ions—It has been long recognized that divalent cations such as Ca²⁺ and Mg²⁺ in the cell culture media can act as an effective bridge to bind negatively charged BSA protein molecules to negatively charged surfaces of TiO₂, metal or hydroxyapatite nanoparticles (22, 25–26). In a very recent study, reduced protein and Ca²⁺ concentrations in DMEM upon the addition of metal oxide nanoparticles was also observed and attributed to the protein adsorption onto metal oxide nanoparticles through Ca²⁺ cations (27). It is believed that the effective bridging of these divalent cations between BSA and TiO₂ nanoparticle surface has also contributed to the improved TiO₂ nanoparticle dispersion in this investigation. The relatively poorer dispersion in the LB medium could be due to the very weak negative charges on TiO₂ surface at a pH of 6.8. Therefore, only at a very high BSA concentration, i.e., 5 mg mL⁻¹, a reasonable amount of protein molecules were adsorbed and enough steric or electrosteric force could be achieved to obtain improved TiO₂ nanoparticle dispersion (Figure 3). It was hypothesized that the Ca²⁺ bridging effect diminished in TBS mainly due to the relatively higher phosphate ion concentration in this medium (Table S1). Since phosphate ions have much higher affinity than the carboxyl groups of BSA for Ca²⁺ site (22), phosphate might compete with BSA for the adsorption on TiO₂ nanoparticle surface. Increasing phosphate concentration usually results in a decrease in BSA adsorption. Boonsongrit *et al.* (28) reported a nearly 70% release of BSA from hydroxyapatite microspheres in half an hour in the presence of 10 mM phosphate. Yang and Zhang (29) showed that pre-adsorption of phosphate ions could also prevent the adsorption of BSA onto hydroxyapatite particle surface. BSA adsorbed on metal (e.g., Ag, Ti) or metal oxide (e.g., Al₂O₃, TiO₂) nanoparticles also showed similar desorption profiles of proteins in the presence of Na₂HPO₄ (21, 30). The desorption process seems to be dependent on pH as well as the BSA concentration. Together with those studies, the results obtained in the present investigation indicate the important role that phosphate ions play in the adsorption/desorption process of BSA and consequently the stability of the TiO₂ nanoparticle suspension.

According to the water chemistry analysis (Table S1), BEGM and TSB are very similar media except that the phosphate ion concentration in BEGM is much lower. To determine if the high phosphate ion concentration would be responsible for the poor dispersion in TSB, the phosphate ion concentration in BEGM was adjusted to the same level (1078 mg L⁻¹) as that in TSB by adding K₂HPO₄. High throughput DLS analysis showed that the TiO₂ agglomerate size gradually increased with increasing phosphate concentration in BEGM (Figure 4). The increased agglomeration could be partly due to the lower charge of phosphate ions as compared to that of BSA at the same pH, which led to a decrease in electrostatic repulsion between TiO₂ nanoparticles. Since pK_a for H₂PO₄⁻ is 7.2, it is expected that -1 (H₂PO₄⁻) and -2 (HPO₄²⁻) charged phosphate ion species coexist at the pH of 7.4; whereas the BSA molecule carries more than ten negative charges at this pH (22). Another reason could be the much smaller size of phosphate ions, and thus, very little steric stabilizing effect. The strong dependence of particle size on phosphate ion concentration in BEGM suggests that high phosphate ion concentration was an important factor, if not the only one that contributed to the poor dispersing ability of BSA in TSB. No noticeable particle size increase was observed in the SD medium with phosphate ion concentration increased up to 1078 mg L⁻¹ (Figure 4). The small effect of phosphate on TiO₂ nanoparticle dispersibility again indicates the stronger binding of BSA on TiO₂ surface, in agreement with the previously proposed different BSA adsorption mechanism in this medium.

Synergistic Effect of Proteins in FBS—For the FBS used in this study, BSA constitutes 16.4 mg mL⁻¹ of the total NPS protein content that amounts to 39.5 mg mL⁻¹.

Therefore the 10% of FBS concentration contains 1.64 mg mL^{-1} of BSA. When this concentration was used, highly dispersed TiO_2 nanoparticles with an average hydrodynamic diameter of 200–300 nm were obtained in all media. By varying FBS concentration at a constant TiO_2 concentration ($50 \text{ } \mu\text{g mL}^{-1}$), it was found that 1% FBS was already sufficient to achieve highly dispersed TiO_2 suspension in all media (Figure 5a). The high dispersing ability of FBS makes it a generally useful dispersing agent for stabilizing TiO_2 and potentially other nanoparticles in all different media.

The much better dispersing ability of FBS also suggests that components other than BSA in the serum might have also contributed to the improved dispersion. Since serum is a very complex system containing thousands of different proteins, which may all compete for limited space on nanoparticle surfaces, it is impossible to identify every single protein that has been adsorbed onto a TiO_2 nanoparticle's surface. According to Dawson and co-workers (13, 14), the types of proteins being adsorbed on nanoparticles at any given time are determined by the concentrations of these proteins as well as the binding affinity of each protein for the particular nanoparticle. Proteins with high concentrations and high association rate constants will initially bind to nanoparticle surface, but might be replaced by proteins of lower concentration but higher affinity later on (13). Although the identification of the protein corona composition was not the focus of this investigation, the kinetic behavior of proteins reported by Dawson and co-workers (13, 14) suggests a potential supplementary effect of different proteins towards TiO_2 nanoparticle dispersion. To illustrate this effect, a simple “FBS mimic” protein cocktail containing BSA, γ -globulin, and apo-transferrin was prepared. BSA was selected because it is the most abundant protein in plasma and its concentration is 16.4 mg mL^{-1} in the FBS used in this study. Globulin, another major protein in FBS (31), was also included in the “FBS mimic” protein cocktail. Transferrin as the third important protein was selected even though normally its concentration was relatively low ($1.8\text{--}2.2 \text{ mg mL}^{-1}$) compared to the other two (32). Figure 5b shows the effect of different protein combinations on TiO_2 nanoparticle dispersion in all six cell culture media. When one or two proteins were used, improved nanoparticle dispersion was observed in some, but not all media. Only when a mixture of all three proteins was used, a universally improved dispersion was obtained in all media. Although in most media the particle sizes are slightly larger compared to those obtained using FBS, the result clearly demonstrated a synergistic effect of these three proteins on TiO_2 nanoparticle dispersion, therefore explained the high dispersing ability of FBS.

Stability Evaluation of TiO_2 Nanoparticle Dispersions

High throughput DLS and UV-vis analysis were used as two parallel methods for the stability studies. Most agglomeration kinetics studies were conducted using the built-in kinetics feature in the HT-DLS instrument. This method could not be used for the media without any dispersing agents. Because the large agglomerates settled rapidly at the bottom of the wells, caused severe light scattering, led to frequent detector turning-off, and made the measurements impossible. As an alternative method, a larger quantity ($\sim 5 \text{ mL}$) of TiO_2 nanoparticle suspension with a $50 \text{ } \mu\text{g mL}^{-1}$ concentration was prepared in a glass sample vial; samples were taken at one-hour time intervals and were vortexed for $\sim 10 \text{ s}$ immediately before analysis. Figure 6 shows that in these dispersing-agent-free media all particles remained in the 700–1000 nm size range during the 24 hour kinetics study. The similar particle size implies that sedimentation rather than particle agglomeration dominates for particle collision in this size regime. This was confirmed by the sedimentation study (Figure S2), which showed poor TiO_2 nanoparticle stability in all six media. At a $50 \text{ } \mu\text{g mL}^{-1}$ initial concentration, only $1\text{--}7 \text{ } \mu\text{g mL}^{-1}$ of TiO_2 nanoparticles was left in the supernatant after 24 hours (Figure S2 and Table 2).

In agreement with the dispersion results, both the agglomeration kinetics (Figure 6) and the sedimentation study (Table 2) showed that the stability of the TiO₂ nanoparticle dispersions were greatly improved with the aid of BSA, especially in DMEM, SD, and YPD media. The only exceptions were in LB and TSB, in which large TiO₂ agglomerates existed and the suspension showed lower stability. Fetal bovine serum, which led to the best TiO₂ nanoparticle dispersion, also exhibited the highest stabilizing ability. Both HT-DLS (Figure 6) and UV-vis (Table 2) analyses showed that a FBS concentration as low as 1% was sufficient to achieve highly stable TiO₂ nanoparticle suspensions.

In summary, TiO₂ P25 nanoparticles tend to agglomerate into much larger size (700–1052 nm) than their primary sizes when directly suspended in cell culture media. Bovine serum albumin greatly improved the nanoparticle dispersion in most media. However the effectiveness varied from medium to medium, mainly due to the different water chemistries, and thus, different protein-nanoparticle interaction mechanisms in the media. Phosphate ions play an important role in the nanoparticle dispersion. The results of the studies on phosphate ion effect provide valuable guidance for preparing nanoparticle suspensions during *in vitro* or *in vivo* toxicity studies. FBS appeared to be the best dispersing agent of these studies for stabilizing TiO₂ nanoparticles in all six cell culture media, which was attributed to the synergistic effect of various proteins in FBS. This synergistic effect was successfully demonstrated in a simple “FBS mimic” protein cocktail containing BSA, γ -globulin, and apo-transferrin.

Supplementary Material

Refer to Web version on PubMed Central for supplementary material.

Acknowledgments

This work is supported by the National Science Foundation and the Environmental Protection Agency under Cooperative Agreement Number EF 0830117. Any opinions, findings, conclusions or recommendations expressed herein are those of the author(s) and do not necessarily reflect the views of the National Science Foundation or the Environmental Protection Agency. This work has not been subjected to an EPA peer and policy review. Key support was also provided by the UC Lead Campus for Nanotoxicology Training and Research, funded by UC TSR&TP, and the US Public Health Service Grants, RO1 ES016746, and RC2ES018766.

Literature Cited

1. Nel A, Xia T, Madler L, Li N. Toxic potential of materials at the nanolevel. *Science*. 2006; 311(5761):622–627. [PubMed: 16456071]
2. Powers KW, Brown SC, Krishna VB, Wasdo SC, Moudgil BM, Roberts SM. Research strategies for safety evaluation of nanomaterials. Part VI. Characterization of nanoscale particles for toxicological evaluation. *Toxicol Sci*. 2006; 90(2):296–303. [PubMed: 16407094]
3. Sager TM, Porter DW, Robinson VA, Lindsley WG, Schwegler-Berry DE, Castranova V. Improved method to disperse nanoparticles for *in vitro* and *in vivo* investigation of toxicity. *Nanotoxicology*. 2007; 1(2):118–129.
4. Bihari P, Vippola M, Schultes S, Praetner M, Khandoga AG, Reichel CA, Coester C, Tuomi T, Rehberg M, Krombach F. Optimized dispersion of nanoparticles for biological *in vitro* and *in vivo* studies. *Particle and Fibre Toxicology*. 2008; 5:14. [PubMed: 18990217]
5. Porter D, Sriram K, Wolfarth M, Jefferson A, Schwegler-Berry D, Andrew M, Castranova V. A biocompatible medium for nanoparticle dispersion. *Nanotoxicology*. 2008; 2(3):144–154.
6. Elgrabli D, Abella-Gallart S, Aguerre-Chariol O, Robidel F, Rogerieux F, Boczkowski J, Lacroix G. Effect of BSA on carbon nanotube dispersion for *in vivo* and *in vitro* studies. *Nanotoxicology*. 2007; 1(4):266–278.

7. George S, Pokhrel S, Xia T, Gilbert B, Ji ZX, Schowalter M, Rosenauer A, Damoiseaux R, Bradley KA, Madler L, Nel AE. Use of a Rapid Cytotoxicity Screening Approach To Engineer a Safer Zinc Oxide Nanoparticle through Iron Doping. *Acs Nano*. 2010; 4(1):15–29. [PubMed: 20043640]
8. Xia T, Kovoichich M, Liong M, Madler L, Gilbert B, Shi HB, Yeh JI, Zink JI, Nel AE. Comparison of the Mechanism of Toxicity of Zinc Oxide and Cerium Oxide Nanoparticles Based on Dissolution and Oxidative Stress Properties. *Acs Nano*. 2008; 2(10):2121–2134. [PubMed: 19206459]
9. Chithrani BD, Ghazani AA, Chan WCW. Determining the size and shape dependence of gold nanoparticle uptake into mammalian cells. *Nano Letters*. 2006; 6(4):662–668. [PubMed: 16608261]
10. Kneipp J, Kneipp H, McLaughlin M, Brown D, Kneipp K. In vivo molecular probing of cellular compartments with gold nanoparticles and nanoaggregates. *Nano Letters*. 2006; 6(10):2225–2231. [PubMed: 17034088]
11. Nishikawa T, Iwakiri N, Kaneko Y, Taguchi A, Fukushima K, Mori H, Morone N, Kadokawa J. Nitric Oxide Release in Human Aortic Endothelial Cells Mediated by Delivery of Amphiphilic Polysiloxane Nanoparticles to Caveolae. *Biomacromolecules*. 2009; 10(8):2074–2085. [PubMed: 19583242]
12. Nativo P, Prior IA, Brust M. Uptake and intracellular fate of surface-modified gold nanoparticles. *Acs Nano*. 2008; 2(8):1639–1644. [PubMed: 19206367]
13. Cedervall T, Lynch I, Foy M, Berggard T, Donnelly SC, Cagney G, Linse S, Dawson KA. Detailed identification of plasma proteins adsorbed on copolymer nanoparticles. *Angewandte Chemie-International Edition*. 2007; 46(30):5754–5756.
14. Lynch I, Dawson KA. Protein-nanoparticle interactions. *Nano Today*. 2008; 3(1–2):40–47.
15. Jiang J, Oberdörster G, Biswas P. Characterization of size, surface charge, and agglomeration state of nanoparticle dispersions for toxicological studies. *J Nanopart Res*. 2009; 11(1):77–89.
16. Braydich-Stolle LK, Schaeublin NM, Murdock RC, Jiang J, Biswas P, Schlager JJ, Hussain SM. Crystal structure mediates mode of cell death in TiO₂ nanotoxicity. *J Nanopart Res*. 2009; 11(6):1361–1374.
17. Derjaguin BV, Landau LD. Theory of the stability of strongly charged lyophobic sols and of the adhesion of strongly charged particles in solutions of electrolytes. *Acta Physicochim URSS*. 1941; 14:733–762.
18. Israelachvili, JN. *Intermolecular and Surface Forces*. 2. Academic Press; London: 1992.
19. Patil S, Sandberg A, Heckert E, Self W, Seal S. Protein adsorption and cellular uptake of cerium oxide nanoparticles as a function of zeta potential. *Biomaterials*. 2007; 28(31):4600–4607. [PubMed: 17675227]
20. Wassell DTH, Hall RC, Embery G. Adsorption of bovine serum-albumin onto hydroxyapatite. *Biomaterials*. 1995; 16(9):697–702. [PubMed: 7578773]
21. Wassell DTH, Embery G. Adsorption of bovine serum albumin on to titanium powder. *Biomaterials*. 1996; 17(9):859–864. [PubMed: 8718930]
22. Giacomelli CE, Avena MJ, Pauli CPD. Adsorption of bovine serum albumin onto TiO₂ particles. *J Colloid Interface Sci*. 1997; 188(2):387–395.
23. Oliva FY, Avalle LB, Cámara OR, Pauli CPD. Adsorption of human serum albumin (HAS) onto colloidal TiO₂ particles, Part I. *J Colloid Interface Sci*. 2003; 261(2):299–311. [PubMed: 16256535]
24. Kopac T, Bozgeyik K, Yener J. Effect of pH and temperature on the adsorption of bovine serum albumin onto titanium oxide. *Colloid Surface A*. 2008; 322(1–3):19–28.
25. Ellingsen JE. A study on the mechanism of protein adsorption to TiO₂. *Biomaterials*. 1991; 12(6):593–596. [PubMed: 1663394]
26. Klinger A, Steinberg D, Kohavi D, Sela MN. Mechanism of adsorption of human albumin to titanium in vitro. *J Biomed Mater Res*. 1997; 36(3):387–392. [PubMed: 9260109]
27. Horie M, Nishio K, Fujita K, Endoh S, Miyauchi A, Saito Y, Iwahashi H, Yamamoto K, Murayama H, Nakano H, Nanashima N, Niki E, Yoshida Y. Protein adsorption of ultrafine metal oxide and its influence on cytotoxicity toward cultured cells. *Chem Res Toxicol*. 2009; 22(3):543–553. [PubMed: 19216582]

28. Boonsongrit Y, Abe H, Sato K, Naito M, Yoshimura M, Ichikawa H, Fukumori Y. Controlled release of bovine serum albumin from hydroxyapatite microspheres for protein delivery system. *Mat Sci Eng B-Solid*. 2008; 148(1–3):162–165.
29. Yang Z, Zhang C. Adsorption/desorption behavior of protein on nanosized hydroxyapatite coatings: a quartz crystal microbalance study. *Appl Surf Sci*. 2009; 255(8):4569–4574.
30. Williams RL, Williams DF. Albumin adsorption onto metal surfaces. *Biomaterials*. 1988; 9(3): 206–212. [PubMed: 3408789]
31. Menza B, Knerr R, Göpferich A, Steinem C. Impedance and QCM analysis of the protein resistance of self-assembled PEGylated alkanethiol layers on gold. *Biomaterials*. 2005; 26(20): 4237–4243. [PubMed: 15683646]
32. Kakuta K, Orino K, Yamamoto S, Watanabe K. High levels of ferritin and its iron in fetal bovine serum. *Comp Biochem Physiol*. 1997; 118(1):165–169.

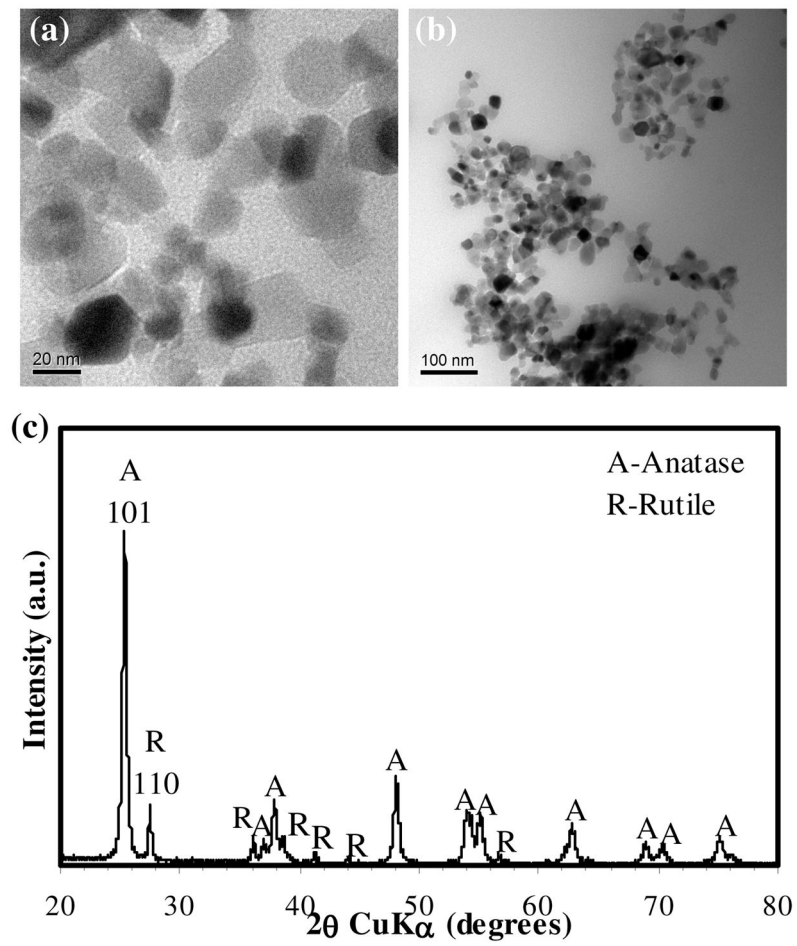


Figure 1. (a, b) TEM images and (c) XRD pattern of Degussa TiO₂ P25 nanoparticles.

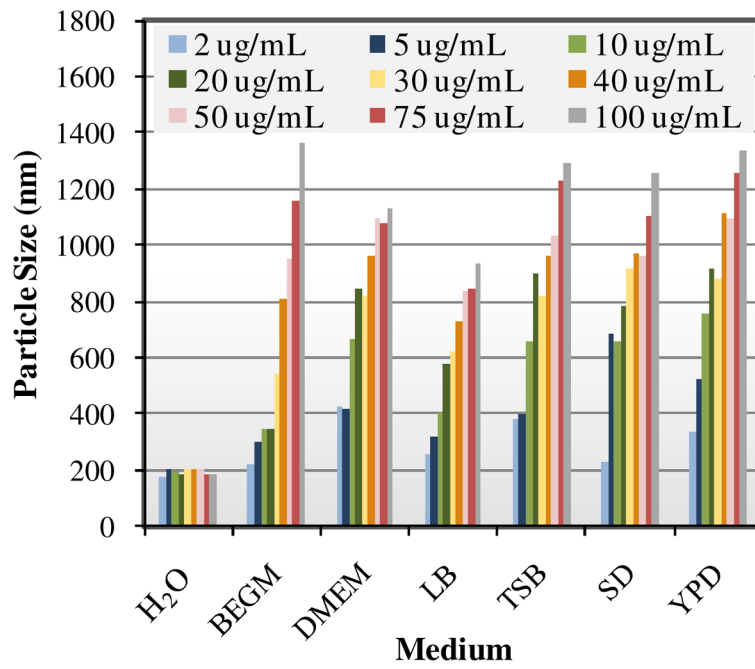


Figure 2. TiO₂ agglomerate size as determined by HT-DLS analysis increased with increasing TiO₂ nanoparticle concentration in all six cell culture media.

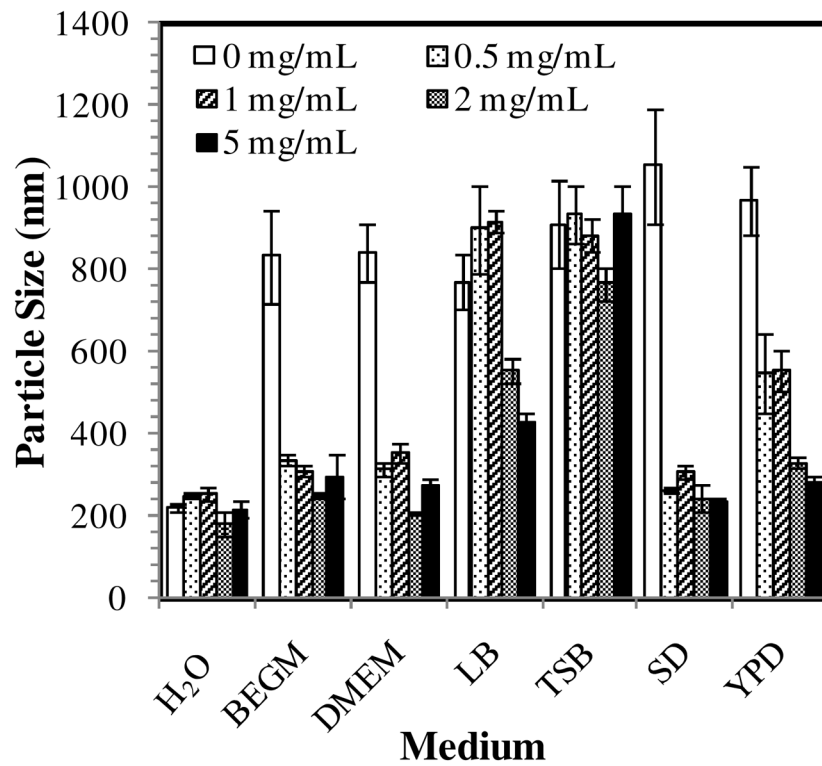


Figure 3. Effect of BSA on TiO₂ nanoparticle dispersion in water and six different cell culture media. TiO₂ concentration was 50 μg mL⁻¹ in all media.

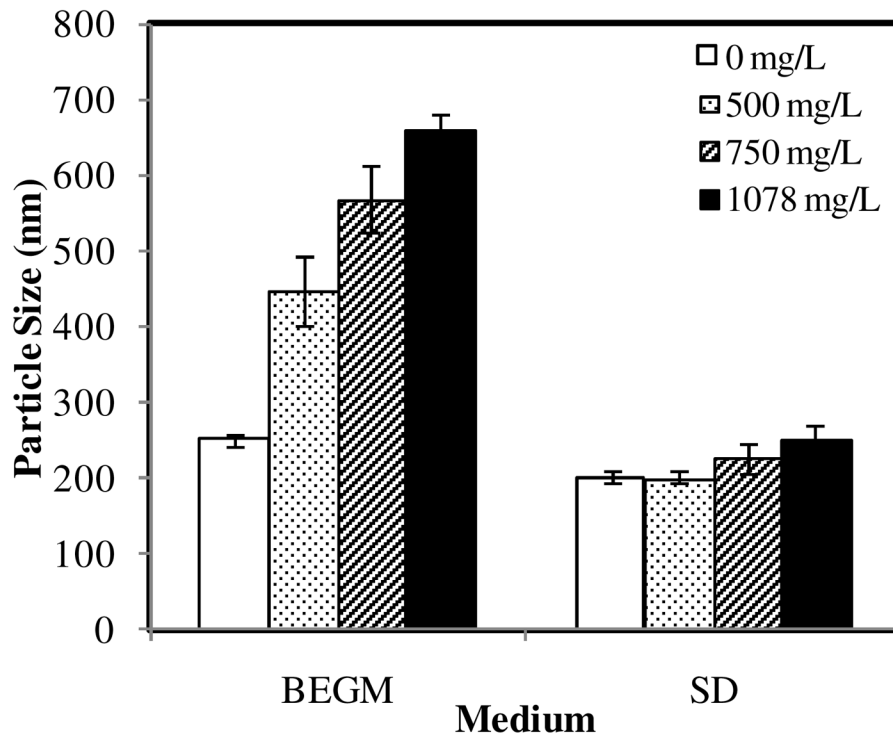


Figure 4. Effect of phosphate ion concentration on TiO₂ nanoparticle dispersion in BEGM and SD with a TiO₂ nanoparticle concentration of 50 μg mL⁻¹.

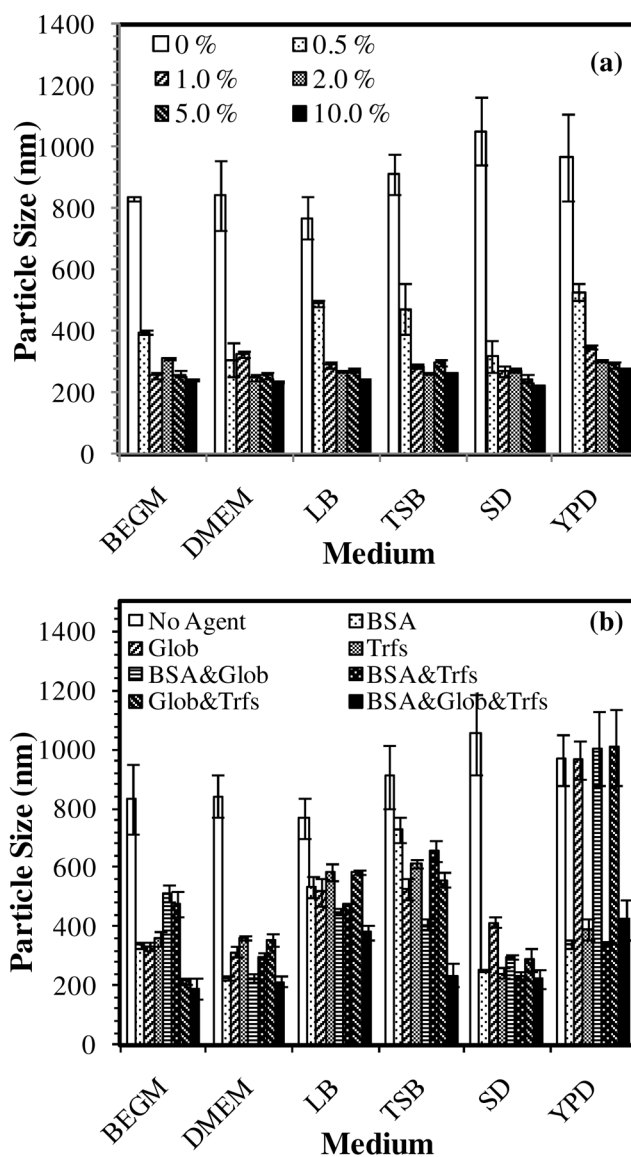


Figure 5. Effect of (a) FBS (0–10% concentration) and (b) protein cocktail containing BSA, γ -globulin (Glob), and Apo-transferrin (Trsf), on TiO₂ nanoparticle dispersion. In (b), when only one protein was added, a 2 mg mL⁻¹ concentration was used; when a protein mixture was added, each protein had a 1 mg mL⁻¹ concentration. TiO₂ concentration was kept at 50 μ g mL⁻¹ in all experiments.

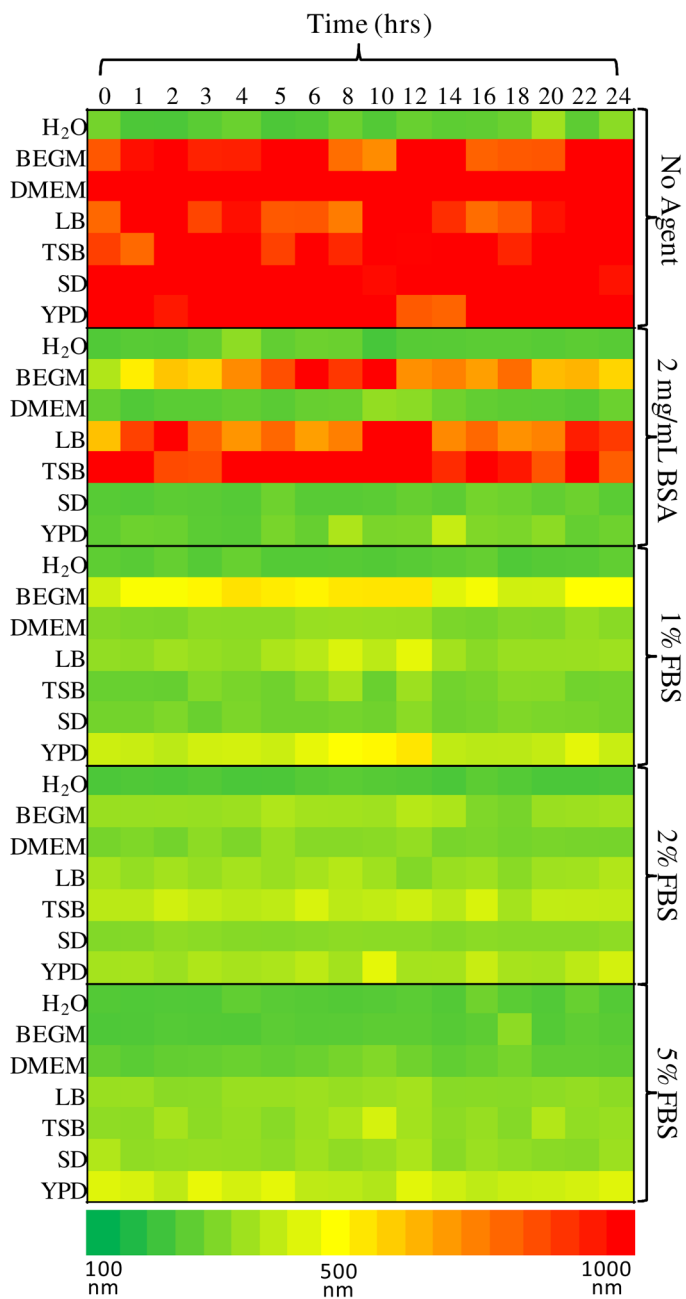


Figure 6. Agglomeration kinetics of TiO₂ nanoparticles in water and various cell culture media at a 50 μg mL⁻¹ TiO₂ concentration.

Table 1

Hydrodynamic diameter (d_H), polydispersity index (PdI), zeta potential (ζ), electrophoretic mobility (EPM), and pH measurements of TiO₂ nanoparticles in cell culture media at a 50 $\mu\text{g mL}^{-1}$ TiO₂ concentration.

Parameter Medium	d_H (nm)	PdI	ζ (mV)	EPM ($\mu\text{mcm/Vs}$)	pH
H ₂ O	209 \pm 9	0.035	30.2 \pm 0.6	2.36	6.1
BEGM	833 \pm 115	0.065	-9.4 \pm 0.8	-0.74	7.6
DMEM	843 \pm 69	0.021	-7.4 \pm 2.5	-0.49	7.5
LB	770 \pm 67	0.017	-14.0 \pm 1.7	-0.94	6.8
TSB	910 \pm 108	0.023	-13.7 \pm 0.4	-0.92	7.3
SD	1052 \pm 139	0.039	-9.4 \pm 0.7	-0.63	4.6
YPD	966 \pm 83	0.025	-12.8 \pm 0.4	-0.86	5.9

Table 2

TiO₂ nanoparticle concentration after 24 hour sedimentation in water and six different cell culture media with or without dispersing agents. The initial TiO₂ concentration is 50 μg mL⁻¹ in all experiments.

	TiO ₂ Concentration (μg/mL)					
	No Agent	2 mg mL ⁻¹ BSA	1.0% FBS	2.0% FBS	5.0% FBS	5.0% FBS
H ₂ O	33.4	43.5	43.2	45.0	47.1	47.1
BEGM	1.6	23.5	33.6	44.5	44.1	44.1
DMEM	6.7	43.6	44.1	47.8	47.3	47.3
LB	4.5	5.2	38.1	44.1	46.9	46.9
TSB	2.1	3.4	34.7	42.5	46.7	46.7
SD	2.8	45.7	42.8	44.1	48.4	48.4
YPD	1.0	40.0	38.9	40.3	46.2	46.2